Temperature Control and Thermal Dosimetry by Microwave Radiometry in Hyperthermia

Luc Dubois, Jean-Pierre Sozanski, Virginie Tessier, Jean-Christophe Camart, Jean-Jacques Fabre, Joseph Pribetich, and Maurice Chivé

Abstract—**This paper presents a synthesis of works undertaken by the Hyperthermia Group of Lille (France) concerning the utilization of the microwave radiometry for the temperature control in hyperthermia therapy. This technique of noninvasive temperature control within the biological tissues has been integrated on many hyperthermia systems now commercialized. We describe the principle of a new radiometer as well as the calculation of radiometric signals. They allow a noninvasive determination of thermal maps inside tissues during the hyperthermia treatments. Many comparisons between theory and experiment have validated our models of thermal dosimetry whose provide a quantitative guidance for the planning of hyperthermia treatments.**

I. Introduction

HUMAN tissues spontaneously emit electromagnetic radiations of thermal origin which can be measured by a very sensitive receiver called "a radiometer" [1] and [2]. When this measurement is carried out in the microwave frequency range, it is possible to evaluate the tissues temperature. Microwave radiometry is used to detect thermal anomalies inside the human body (for example, the detection of breast cancer) [1] and [3], but also to evaluate, noninvasively, the temperature distribution in biological tissues [4]–[6].

Since 1980, the Hyperthermia Group of Lille (composed of the "Circuits et Applicateurs" Research group of the Département Hyperfréquences et Semiconducteurs of IEMN, the Centre Anti-Cancer Oscar Lambret and the Unit 279 INSERM) has developed many hyperthermia systems combining microwave radiometers [6]–[10]. It has been demonstrated that these techniques made it possible to monitor hyperthermia systems, as well as, to plot thermal maps in clinical context in order to optimize forthcoming hyperthermia sessions.

II. Physical Principles of Microwave Radiometry

Any dissipative body emits spontaneous electromagnetic radiations of thermal origin. In the microwave domain, the thermal noise power emitted by the body is directly proportional to the temperature and can be obtained by integrating the spectrum brightness $B(f)$ (i.e., energy radiated per unit of apparent surface and per unit of solid angle).

Manuscript received October 12, 1995; revised February 22, 1996.

L. Dubois, V. Tessier, J.-C. Camart, J.-J. Fabre, and J. Pribetich are with the IEMN-DHS UMR CNRS 9929, Université des Sciences et Technologies de Lille, 59652 Villeneuve D'Ascq Cedex, France.

J.-P. Sozanski is with the INSERM U 279, 59019 Lille Cedex, France.

M. Chivé is with the IEMN-DHS UMR CNRS 9929, Université des Sciences et Technologies de Lille, 59652 Villeneuve D'Ascq Cedex, France. He is also with the INSERM U 279, 59019 Lille Cedex, France.

Publisher Item Identifier S 0018-9480(96)07022-6.

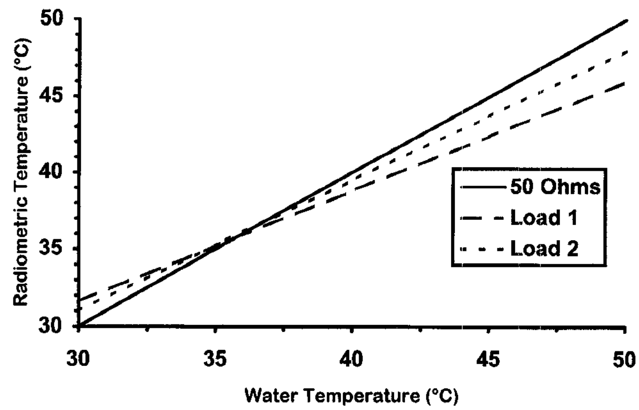

Fig. 1. Calibration curves of a classical radiometer obtained for different loads replacing the applicator. 50 Ω load (ρ = 0 0); Load 1 (ρ = 0.25); Load 2 (ρ = 0.1).

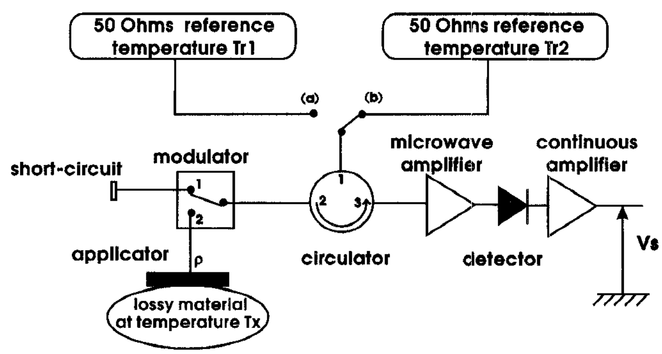

Fig. 2. Structure of the new radiometer with two internal temperature references.

If $T > 10$K, at a frequency f and for a bandwith of 1 Hz, $B(f)$ is expressed by the Rayleigh–Jeans relation

$$B(f) = \frac{2 \cdot f^2 \cdot k_B \cdot T}{c^2} \approx A \cdot T$$

with

k_B Boltzmann's constant ($1.38 \cdot 10^{-23}$ J $\cdot$ K^{-1});
c speed of light ($3 \cdot 10^8$ m $\times$ s^{-1});
T absolute temperature of the body (Kelvins).

The temperature of a dissipative body can thus be determined by a measurement of the electromagnetic power radiated in a given frequency bandwidth. This measurement is achieved by radiometric systems which use an antenna as an electromagnetic power captor in the microwave region. Let

0018–9480/96$05.00 © 1996 IEEE

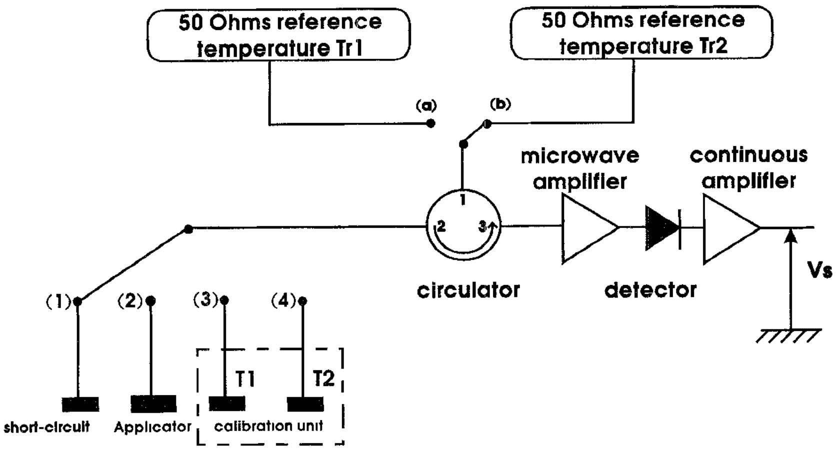

Fig. 3. Structure of the new radiometer containing a calibration unit constituted by two external calibrated sources raised, respectively, to temperature T_1 and T_2.

us consider an antenna put on a dissipative body raised to a uniform temperature T. The power collected by the antenna in a bandwidth Δf is given by Nyquist's formula

$$P = (1-\rho) \cdot k_B \cdot T \cdot \Delta f$$

with

k_B Boltzmann's constant;
T absolute temperature of the body (Kelvins);
ρ power reflection coefficient at the interface applicator-lossy media.

III. Microwave Radiometric Systems for Biomedical Applications

With the first generation of radiometers [1] and [2] the output signal S is proportional to the difference in temperature $(T_x - T_r)$

$$S = G \cdot k_B \cdot \Delta f \cdot (1-\rho) \cdot (T_x - T_r)$$

with

ρ power reflection coefficient at the interface applicator-lossy material;
T_x temperature to measure;
T_r reference temperature;
G gain of the chain.

We note that the output signal S depends on the gain G and on the reflection coefficient ρ. Moreover, a preliminary calibration of the system radiometer-applicator is necessary to obtain the T_x information. The calibration is carried out by putting the applicator in contact with a liquid emissive medium (salt water or physiological serum) that simulates the biological tissues, whose temperature T is made to vary. Then we get a calibration curve $S_{rad} = f(T)$. This calibration procedure takes about twenty minutes.

But the calibration curve depends on the coefficient ρ. The Fig. 1 shows its influence when the applicator is replaced by different microwave loads. Consequently, we have studied a new radiometer allowing to free from the reflection coefficient ρ and from the gain G.

A. Principle of the Ideal Radiometer with Two Internal Temperature References

The structure of this radiometer is given on the Fig. 2. It contains two reference sources constituted by 50 Ω coaxial loads, raised, respectively, to temperature T_{r1} and T_{r2}. A microwave switch allows to select one of these two internal temperature references.

When the switch is in state "a," the continuous voltage at the amplifier output is as follows:

1) modulator in state 1:

$$V_{11} = G \cdot k_B \cdot \Delta f \cdot T_{r1} \tag{1}$$

2) modulator in state 2:

$$V_{12} = G \cdot k_B \cdot \Delta f \cdot [(1-\rho) \cdot T_x + \rho \cdot T_{r1}]. \tag{2}$$

When the switch is in state "b," we obtain

1) modulator in state 1:

$$V_{21} = G \cdot k_B \cdot \Delta f \cdot T_{r2} \tag{3}$$

2) modulator in state 2:

$$V_{22} = G \cdot k_B \cdot \Delta f \cdot [(1-\rho) \cdot T_x + \rho \cdot T_{r2}]. \tag{4}$$

From these relations, we deduce the expression of the reflection coefficient ρ and the expression of the temperature T_x

$$\rho = \frac{V_{12} - V_{22}}{V_{11} - V_{21}}$$

$$T_x = \frac{(V_{11} - V_{12}) \cdot T_{r2} - (V_{21} - V_{22}) \cdot T_{r1}}{V_{11} - V_{12} - V_{21} + V_{22}}. \tag{5}$$

The value of the temperature T_x thus calculated is now independant of the amplifier gain G and of the reflection coefficient ρ. The value T_x represents the radiometric temperature (called T_{rad}) of the lossy material. It is an "average temperature" of the volume of material coupled to the applicator in the radiometer bandwidth. In the particular case of uniform temperature, we have $T_{rad} = T_x$.

The resolution on the determination of the reflection coefficient and for the radiometer sensitivity are given, respectively, by

$$\Delta\rho = \Delta T \cdot \left[\frac{(1+\rho)}{T_{r2} - T_{r1}}.\right] \tag{6}$$

TABLE I
DETERMINATION (WITH THE NEW RADIOMETER) OF THE REFLECTION COEFFICIENT OF DIFFERENT MICROWAVE LOADS REPLACING THE APPLICATOR $\Delta\rho$ IS DETERMINED EXPERIMENTALLY BY A STANDARD DEVIATION CALCULATION

Loads	50 Ω	Load 1	coaxial antenna
ρ (minimum value)	0.018	0.276	0.13
ρ (maximum value)	0.024	0.282	0.138
ρ (average value)	0.021	0.280	0.134
Δρ (experiment)	0.003	0.003	0.004
ρ (theory)	0.0	0.25	-
Δρ (theory)	0.0026	0.0028	-

TABLE II
COMPARISON BETWEEN THE VALUES OF REFLECTION COEFFICIENT DETERMINED WITH THE RADIOMETER, AND SOME NETWORK ANALYZER MEASUREMENTS ACHIEVED IN THE RADIOMETER BANDWIDTH (2–4 GHz)

frequency (GHz)	ρ (network analyser)		ρ (radiometer)	
	Load 1 ρ(theory)=0.25	Load 2 ρ(theory)=0.1	Load 1 ρ(theory)=0.25	Load 2 ρ(theory)=0.1
2.0	0.288	0.125		
2.5	0.288	0.117		
3.0	0.284	0.108	0.280	0.130
3.5	0.283	0.102		
4.5	0.276	0.104		

TABLE III
CHARACTERISTICS OF TWO SETS OF 100 RADIOMETRIC MEASUREMENTS ACHIEVED WHEN THE APPLICATOR IS PUT ON A THERMOSTATED BATH RAISED TO 26.5°C AND THEN TO 45.1°C. ΔT_{rad} IS DETERMINED EXPERIMENTALLY BY A STANDARD DEVIATION CALCULATION

Bath temperature	measurements at 26.5°C	measurements at 45.1°C
Trad (minimum value)	26.52	45.17
Trad (maximum value)	26.78	45.38
Trad (average value)	26.63	45.27
ΔTrad (experiment)	0.058	0.0455
ΔTrad (theory)	0.056	0.036

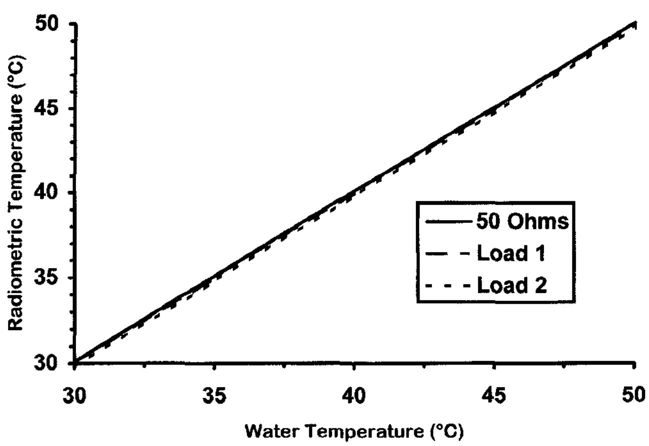

Fig. 4. Calibration curves of the new radiometer, obtained for different loads replacing the applicator. 50 Ω load ($\rho = 0.0$); Load 1 ($\rho = 0.25$); Load 2 ($\rho = 0.1$).

$$\Delta T_x = \Delta T \cdot \frac{|T_{r1} - T_x| - |T_{r2} - T_x|}{(1-\rho) \cdot (T_{r2} - T_{r1})}. \qquad (7)$$

$\Delta T = \sqrt{2} \cdot [(T + T_B)/\sqrt{\Delta f \cdot \tau}]$ is the theoretical sensitivity of the Dicke radiometer [1] and [6] where T_B and τ are, respectively, the chain noise temperature and the time constant of the synchronous detection.

For medical applications the internal temperature references T_{r1} and T_{r2} are raised, respectively, to 34°C and 55°C.

B. Calibration Procedure

In practice, all elements of the radiometer present insertion losses which modify the previous relations (1)–(4). We consider consequently that the radiometer is ideal but with new temperature references noted T_{r1e} and T_{r2e}, deduced from two external calibrated sources raised to temperature T_1 and T_2.

The block diagram of the radiometer is therefore slightly modified in order to include a calibration unit (Fig. 3). The modulator is replaced by a switch with four positions and the ways 3 and 4 are connected to the calibrated sources (well-matched loads with same insertion losses) raised to temperature T_1 and T_2.

To calibrate the radiometer, the four previous operations (1)–(4) are done again but the applicator is now replaced by the well-matched reference loads raised, respectively, to temperature T_1 and T_2. The output voltages are

1) With the unit calibration at temperature T_1:

$$V_{11} = G \cdot k_B \cdot \Delta f \cdot T_{r1};$$
$$V_{12a} = G \cdot k_B \cdot \Delta f \cdot T_1$$
$$V_{21} = G \cdot k_B \cdot \Delta f \cdot T_{r2};$$
$$V_{22a} = G \cdot k_B \cdot \Delta f \cdot T_1$$

2) With the unit calibration at temperature T_2:

$$V_{11} = G \cdot k_B \cdot \Delta f \cdot T_{r1};$$

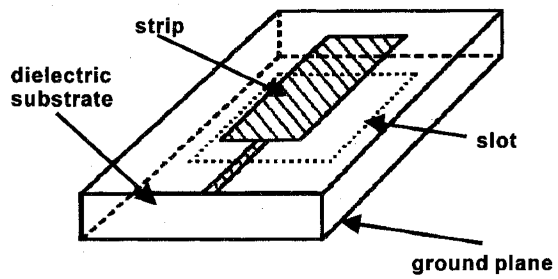

(a)

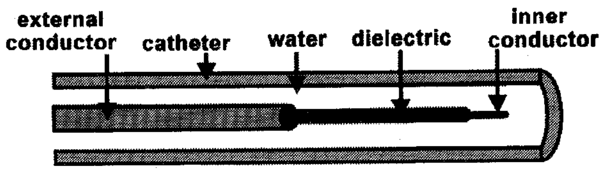

(b)

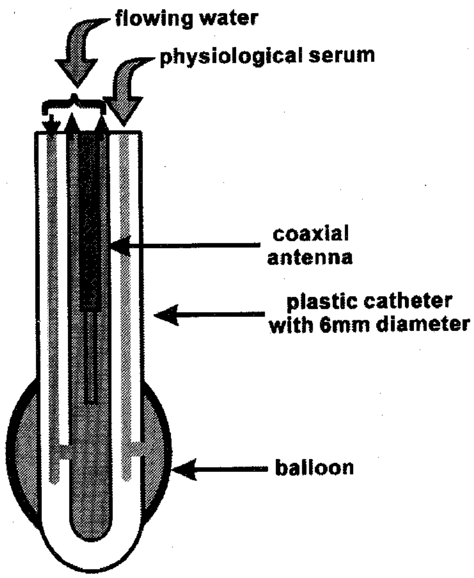

(c)

Fig. 5. View of some applicators used on microwave hyperthermia systems controlled by microwave radiometry. (a) Microstrip-microslot applicator for external hyperthermia, (b) coaxial antenna for interstitial hyperthermia, and (c) endocavitary applicator for prostatic hyperthermia.

$$V_{12b} = G \cdot k_B \cdot \Delta f \cdot T_2$$
$$V_{21} = G \cdot k_B \cdot \Delta f \cdot T_{r2};$$
$$V_{22b} = G \cdot k_B \cdot \Delta f \cdot T_2.$$

By combining these relations with the relation 5, we deduce the expression of the equivalent temperature references T_{r1e} and T_{r2e} as shown in (7a) at the bottom of the page. The radiometric temperature is therefore calculated by means of relation 5 where the values T_{r1} and T_{r2} are replaced by T_{r1e} and T_{r2e}.

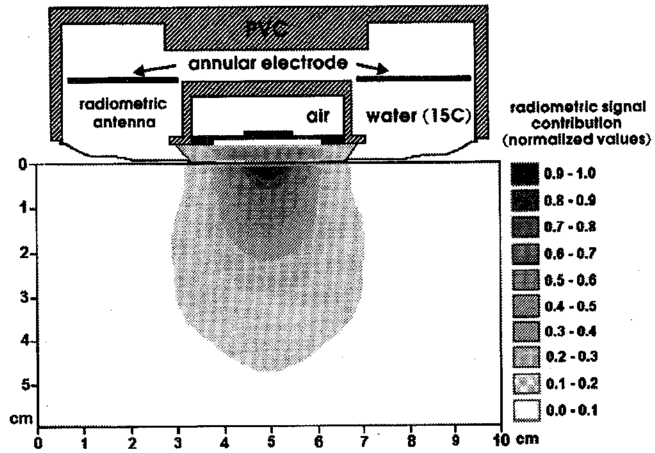

(a)

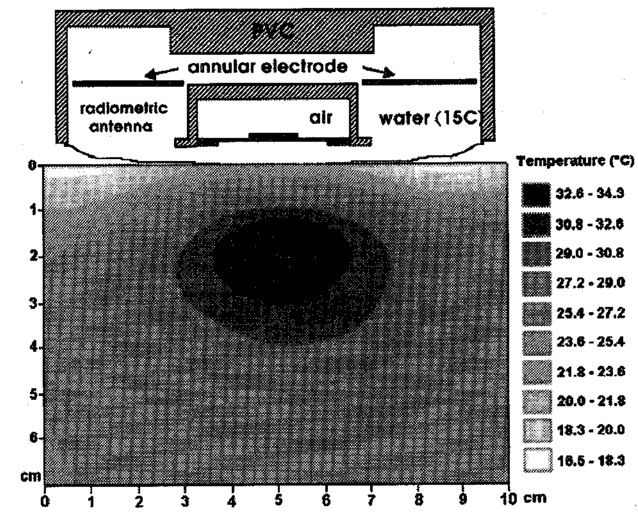

(b)

Fig. 6. Microwave radiometry can also be used in capacitive hyperthermia systems. (a) Normalized radiometric signal contribution of each subvolume [calculated by (8)] and (b) thermal map obtained within an aquasonic gel after 50 min. heating by using a capacitive hyperthermia system ($f = 13.56$ MHz, $P_{inc} = 93$ W) controlled by microwave radiometry (1.1 GHz). The measured and calculated radiometric temperatures are, respectively, 27°C and 27.7°C.

The calibration procedure takes about one min and it is automatic without any modification of the position of the applicator.

To verify and confirm this calibration procedure the applicator has been replaced by loads which present differents values of reflection coefficient. These loads were plunged in a thermostated bath which temperature T is made to vary.

The corresponding calibration curves are presented in Fig. 4. The slope is equal to the unity and varies less than six per thousand when the reflection coefficient ρ varies from 0.03–0.3.

We note therefore a straight improvement with regard to results obtained with classical radiometers.

$$T_{r1e} = \frac{T_1 \cdot (V_{11} - V_{12b}) \cdot (V_{21} - V_{22a} - V_{11} + V_{12a}) - T_2 \cdot (V_{11} - V_{12a}) \cdot (V_{21} - V_{22b} - V_{11} + V_{12a})}{(V_{21} - V_{22a}) \cdot (V_{11} - V_{12b}) - (V_{11} - V_{12a}) \cdot (V_{21} - V_{22b})}$$
$$T_{r2e} = \frac{-T_1 \cdot (V_{21} - V_{22b}) \cdot (V_{21} - V_{22a} - V_{11} + V_{12a}) + T_2 \cdot (V_{21} - V_{22a}) \cdot (V_{21} - V_{22b} - V_{11} + V_{12a})}{-(V_{21} - V_{22a}) \cdot (V_{11} - V_{12b}) + (V_{11} - V_{12a}) \cdot (V_{21} - V_{22b})} \qquad (7a)$$

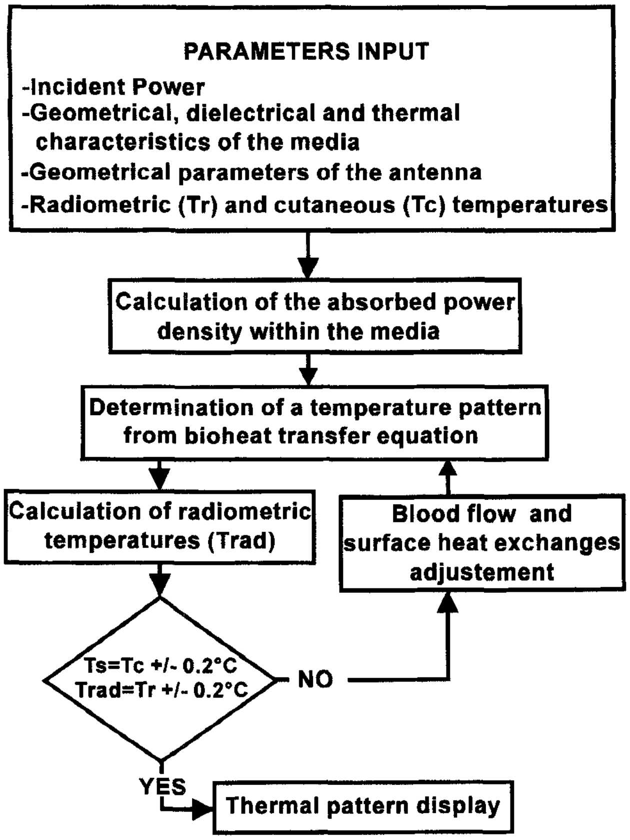

Fig. 7. Flowchart of the thermal dosimetry software.

C. Performance

1) Measurement of the Reflection Coefficient: We have determined, with this new radiometer (which operates in the 2–4 GHz frequency ranges), the reflection coefficient ρ of different microwave loads replacing the applicator (Table I). The values thus determined have been compared with the network analyzer measurements achieved in the radiometer bandwidth (for the same microwave loads). Results show a good agreement between the values measured by the network analyzer and those determined with the radiometer (Table II).

2) Radiometric Temperature Measurements Sensitivity: The sensitivity of the radiometer depends both on the reflection coefficient ρ and on the temperature T_x to be measured. From relation 7 it appears that the best sensitivity is obtained when the temperature is situated between the internal reference temperatures (T_{r1}, T_{r2}) and when the reflection coefficient is equal to zero.

Table III shows the characteristics of two sets of 100 radiometric measurements achieved when the applicator is put on a thermostated bath (which stability temperature is better than 0.02°C) raised to 26.5°C and then to 45.1°C.

The delay for a radiometric measurement is around 5 s. We note that the temperature resolution ΔT_{rad} is better than 0.05°C when the radiometric temperature (T_{rad}) is equal to 45.1°C. The value of ΔT_{rad} increases if T_{rad} is not situated between T_{r1} and T_{r2}.

Experimental values of the temperature resolution are also in good agreement with the theoretical values. So, the behavior of radiometer is therefore completely in agreement with the theoretical analysis.

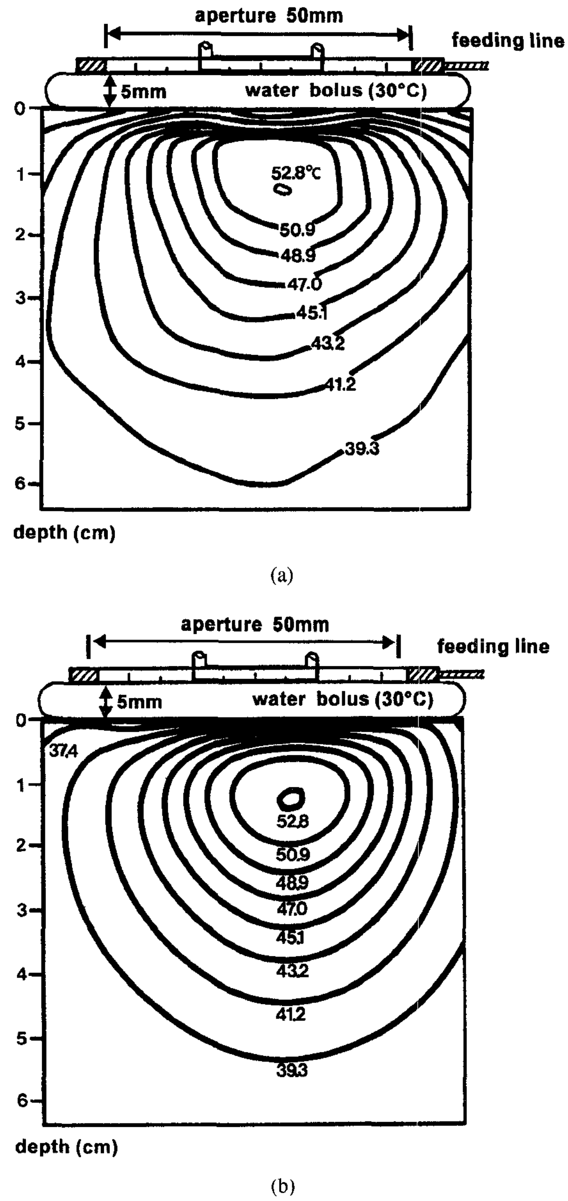

Fig. 8. (a) Thermal profile obtained along the feeding line of a microstrip-microslot applicator (diameter = 50 mm; ε_r = 4.9) laid on a polyacrylamide gel, after 1 h heating (P_{inc} = 8.6 W; f = 915 MHz)—radiometric temperature T_{rad} (3 GHz) = 37.9°C; (b) calculated isotherms in the same conditions—calculated radiometric temperature T_{rad}(3 GHz) = 37.6°C.

IV. Exploitation of Radiometric Signals

Radiometric signals received by a radiometer may be used for detecting thermal anomalies inside biological tissues [1] and [3] or may be used for noninvasive temperature control in hyperthermia treatments [6]–[10]. In the case of microwave hyperthermia, the applicators (Fig. 5) are used both for heating and for radiometric temperature measurements.

From these measurements and from radiometric signals calculation it is also possible to evaluate noninvasively, the temperature distribution inside the biological tissues [4]–[6].

A. Radiometric Signals Calculation

The noise power P_c measured through an applicator by a radiometer centered on a frequency f_R (with a bandwidth Δf) is the integral summation of the elementary noise powers emitted by each subvolume of the dissipative media and multiplied by a weighting coefficient C. This coefficient corresponds to the volume coupled to the applicator which contributes to the noise power received by the radiometer. It depends on the radiative diagram of the applicator at the f_R frequency and on the dielectric properties [11] and [12] of the lossy media

$$P_c = (1 - \rho) \cdot \int_x \int_y \int_z dP(x, y, z) \cdot dx \cdot dy \cdot dz$$

with

$$dP(x, y, z) = C(x, y, z) \cdot k_B \cdot T(x, y, z) \cdot \Delta f$$

and

$$C(x, y, z) = \tfrac{1}{2} \cdot \sigma(x, y, z) \cdot |E(x, y, z)|^2. \tag{8}$$

ρ is the power reflection coefficient in the input of the applicator; E is the electric field inside the lossy media when the applicator is used in active mode at the frequency f_R; and σ is the electrical conductivity of media.

The corresponding radiometric temperature is given by

$$T_{rad} = \frac{\int_x \int_y \int_z C(x, y, z) \cdot T(x, y, z) \cdot dx \cdot dy \cdot dz}{\int_x \int_y \int_z C(x, y, z) \cdot dx \cdot dy \cdot dz}.$$

Thus the radiometer detects an average of the temperature distribution inside media, weighted by the squared electric field pattern of the applicator used as a receiver. The electric field E may be determined from many methods [7], [8], [10], and [13]–[15] and by applying the antenna reciprocity theorem.

For example, we give in Fig. 6(a), the map of weighting coefficients computed in the case of a radiometric antenna used in a hyperthermia capacitive system.

From this calculation we have determined the radiometric temperature corresponding to the thermal map shown in Fig. 6(b). The calculated and measured radiometric temperatures are in good agreement.

B. Application to Thermal Dosimetry

The radiometric signals calculation combined with the resolution of bioheat transfer equation may be used to determine, noninvasively, the thermal map inside tissues during hyperthermia sessions [6]–[8], and [10].

We give in Fig. 7 the flowchart of the thermal dosimetry software [7] and [8]. In order to prove the validity of our modeling, hyperthermia sessions on polyacrylamide gel were first performed. The Fig. 8 shows a great concordance between theoretical and experimental isotherms when a microstrip-microslot applicator [7] and [16] is used for microwave heating.

In the case of microwave hyperthermia on patients (Fig. 9), many hyperthermia sessions have confirmed the good concordance between intratumoral temperatures measured by inserted thermocouples and bidimensional temperature profile reconstruction.

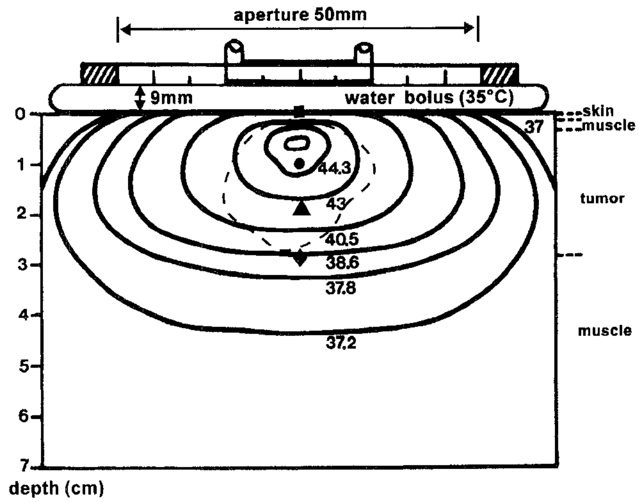

Fig. 9. Comparison between calculated isotherms and temperatures measured by thermocouples on the axis of the applicator (diameter = 50 mm; $\varepsilon_r = 4.9$) during a hyperthermia session on a patient *Experimental data:* $P_{inc} = 21$ W; $f = 915$ MHz, radiometric temperatures T_{rad} (1 GHz) = 40 1°C, T_{rad} (3 GHz) = 38.6°C; temperatures measured by implemented thermocouples: ● 44.3°C; ▲ 43 0°C; ■ 40.5°C; ♦ 38.6°C.

The computations are made on a desktop computer and take a short CPU time (around 3 min.) which demonstrates the possibility of simulation during the hyperthermia session. However, in clinical situation, it's necessary to know accurately the structure of the heated tissues and to use multi-frequency radiometry to improve the retrieval of temperature distributions.

V. Conclusion

The new radiometer with two internal temperature references presents a great advantage as compared to the first generation one (with only one internal reference). Its calibration can be achieved very quickly (only one minute) using two calibrated sources. Another performance is that the radiometer measurement is independent of the reflection coefficient at the applicator-tissues interface.

Microwave radiometry, used routinely since 1984, has proven its efficiency for noninvasive temperature control during hyperthermia treatments. The radiometric signals calculation allows to determine, noninvasively and with a great accuracy, the thermal map within the tissues during hyperthermia sessions. So, our modeling allows to realize a thermal dosimetry and to provide a quantitative guidance for the planning of hyperthermia treatments.

References

[1] D. V Land, "A clinical microwave thermography system," *IEE Proc.*, vol. 134, pt. A, no. 2, pp. 193–200, Feb. 1987

[2] M. Chivé, E. Constant, Y. Leroy, A. Mamouni, Y. Moschetto, D. D. Nguyen, and J. P. Sozanski, "Procédé et dispositif de thermographie-hyperthermie en microondes," Brevet Français déposé le 9 Janvier 1981, no. 8100682.

[3] B. Bocquet, J. C. Van de Velde, A. Mamouni, Y. Leroy, G. Giaux, J. Delannoy, and D. Delvalee, "Microwave radiometric imaging at 3 GHz for the exploration of breast tumors," *IEEE Trans. Microwave Theory Tech.*, vol. 38, pp. 791–793, 1990.

[4] F. Bardati, M. Mongiardo, and D. Solimini, "Retrieval of hyperthermia-induced temperature distribution from noisy microwave radiometric data," *Electron. Lett.*, vol. 21, pp. 800–801, 1985.

[5] ——, "Synthetic array for radiometric retrieval of thermal fields in tissues," *IEEE Trans. Microwave Theory Tech.*, vol. 34, no. 5, pp. 579–583, May 1986.

[6] M. Chivé, "Use of the microwave radiometry for hyperthermia monitoring and as a basis for thermal dosimetry," in *Methods of Hyperthermia Control, Series on Clinical Thermology, Subseries Thermotherapy,* M. Gautherie, Ed. Heidelberg: Springer-Verlag, 1990, vol. 3, pp. 113–125.

[7] L. Dubois, J. Pribetich, J. J. Fabre, M. Chivé, and Y. Moschetto, "Noninvasive microwave multifrequency radiometry used in microwave hyperthermia for bidimensional reconstruction of temperature patterns," *Int. J. Hyperthermia,* vol. 9, no. 3, pp. 415–431, 1993.

[8] J. C. Camart, J. J. Fabre, B. Prevost, J. Pribetich, and M. Chive, "Coaxial antenna array for 915 MHz interstitial hyperthermia: Design and modelization—Power deposition and heating pattern-phased array," *IEEE Trans. Microwave Theory Tech.*, vol. 40, no. 12, pp. 2243–2250, Dec. 1992.

[9] B. Prevost, J. J. Fabre, J. C. Camart, and M. Chivé, "Noninvasive thermometry practice for interstitial hyperthermia," in *Medical Radiology Interstitial and Intracavitary Thermoradiotherapy,* M. H. Seegenschmiedt and R. Sauer, Eds. Heidelberg: Springer-Verlag.

[10] M. Chivé, J. C. Camart, and F. Morganti, "Thermal modeling for intracavitary heating," in *Interstitial and Intracavitary Thermo-radiotherapy,* M. H. Seegenschmiedt and R. Sauer, Eds. Heidelberg: Springer-Verlag, pp. 123–130.

[11] J. L. Scheeps and K. R. Foster, "The U.H.F and Microwave dielectric properties of normal and tumor tissues: Variation in dielectric properties with tissue water content," *Phys. Med. Bio.,* vol. 25, no. 6, pp. 1149–1159, 1980.

[12] M. A. Stuchly and S. S. Stuchly, "Dielectric properties of biological substances-tabulated," *J. Microwave Power,* vol. 15, no. 1, pp. 19–26, 1980.

[13] L. Dubois, J. Bera, J. Pribetich, and M. Chivé, "Theoretical and experimental determination of the power deposition on a microstrip-microslot applicator for biomedical applications," *M.O.T.L.*, vol. 4, no. 4, Mar. 1991.

[14] F. Duhamel, L. Dubois, M. Chivé, and J. Pribetich, "Combining S.D.A. and F.D.T.D methods for modeling of planar applicators used in microwave hyperthermia," *M.O.T.L.*, vol. 7, no. 5, Apr. 1994.

[15] P. Y. Cresson, C. Michel, L. Dubois, M. Chivé, and J. Pribetich, "Complete 3-D modeling of new microstrip-microslot applicators for microwave hyperthermia using the FDTD method," *IEEE Trans. Microwave Theory Tech.*, vol. 42, no. 12, pp. 2657–2666, Dec. 1994.

[16] R. Ledee, M. Chivé, and M. Plancot, "Microstrip-microslot antennas for biomédical applications: Frequency analysis of different parameters of this type of applicator," *Electron. Lett.*, vol. 21, no. 7, pp. 304–305, Mar. 28, 1985.

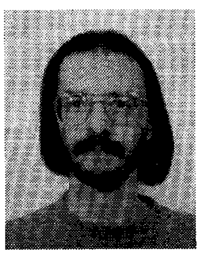

Luc Dubois was born June 6, 1963, in Villers-Guislain, France. He received the M.S. and Ph.D. degrees from the University of Lille in 1987 and 1991, respectively.

He works on the design development and modeling of microwaves sensors for biomedical and industrial applications at the Institut d'Electronique et de Microélectronique du Nord (IEMN) UMR CNRS no. 9929, Department Hyperfréquences and Semiconducteurs. He is currently an Associate Professor at the University of Lille.

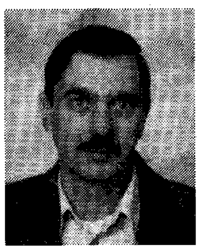

Jean-Pierre Sozanski was born in Poix du Nord, France, on April 5, 1951. He received the Electronic Engineering diploma in 1978 from the "Conservatoire National des Arts et Métiers" of Lille. He received the Ph.D. degree in 1995.

He worked in the Centre U279 INSERM on biomedical applications mainly on the microwave applications: the hyperthermia-thermotherapy systems controlled by microwave radiometry. He now works on other biomedical applications.

Virginie Tessier was born in Douai, France, on December 27, 1971. She received the engineer degree from the Ecole Universitaire Des Ingénieurs de Lille (EUDIL) University of Sciences and Technology of Lille, in 1994. She is now studying for the Ph.D. degree.

She works on microwave sensors for biomedical and industrial applications at the Institut d'Electronique et de Microélectronique du Nord (IEMN). She is also an Assistant Professor at the University of Lens.

Jean-Christophe Camart was born in Lille, France, on April 6, 1963. He received the M.S. degree and the Ph.D. degree from University of Lille in 1990 and 1993, respectively.

He works on applicators for interstitial hyperthermia and endocavitary thermotherapy in the Institut d'Electronique et de Microelectronique du Nord (IEMN). He is currently an Associate Professor at the Ecole Universitaire Des Ingénieurs de Lille (EUDIL) University of Sciences and Technology of Lille.

Jean-Jacques Fabre was born in Lille, France, on April 8, 1952. He received the M.S. degree and the Ph.D. degree from University of Lille in 1979 and 1982, respectively.

He joined the Hyperthermia Group of Lille in 1985 and has devoted full time to the design and development of microwave applicators and systems for interstitial hyperthermia in the Institut d'Electronique et de Microelectronique du Nord (IEMN). He is currently an Associate Professor at the University of Sciences and Technology of Lille.

Joseph Pribetich was born October 31, 1944, in Roubaix, France. He received the Doctorat 3éme Cycle and the Docteur-es-Sciences Physiques degrees from the University of Lille in 1971 and 1979, respectively.

He is working at the Institut d'Electronique et de Microélectronique du Nord (IEMN) UMR CNRS no. 9929, Department Hyperfréquences & Semiconducteurs, on the modeling of applicators and antennas to be used in hyperthermia systems and in industrial applications. He is also a Professor of electronics at the University of Artois.

Maurice Chivé was born in Lille, France, on February 18, 1940. He received the Doctorate 3ème Cycle and the Docteur-es-Sciences Physiques degrees from the University in 1967 and 1978, respectively.

He joined the Centre Hyperfréquences et Semi-conducteurs Université de Lille in 1968, where he was concerned with research on semiconductor devices until 1978. Since then he has been working on biomedical applications of microwaves. He is now Professor at this University, and Research Manager of the Hyperthermia Group of Lille.